HHS Public Access

Author manuscript

Nature. Author manuscript; available in PMC 2015 June 30.

Published in final edited form as:

Nature. 2014 August 14; 512(7513): 185–189. doi:10.1038/nature13402.

Neuropsychosocial profiles of current and future adolescent alcohol misusers

Robert Whelan[1,2], **Richard Watts**[3], **Catherine A. Orr**[4], **Robert R. Althoff**[5,6], **Eric Artiges**[7,8], **Tobias Banaschewski**[9], **Gareth J. Barker**[10], **Arun L. W. Bokde**[11], **Christian Büche**[12,13], **Fabiana M. Carvalho**[10], **Patricia J. Conrod**[10,14], **Herta Flor**[9], **Mira Fauth-Bühler**[9,15], **Vincent Frouin**[16], **Juergen Gallinat**[12,17], **Gabriela Gan**[18], **Penny Gowland**[19], **Andreas Heinz**[17], **Bernd Ittermann**[20], **Claire Lawrence**[21], **Karl Mann**[9], **Jean-Luc Martinot**[7,22], **Frauke Nees**[9], **Nick Ortiz**[1,23], **Marie-Laure Paillère-Martinot**[17,22], **Tomas Paus**[24,25], **Zdenka Pausova**[26], **Marcella Rietschel**[9], **Trevor W. Robbins**[27], **Michael N. Smolka**[18], **Andreas Ströhle**[17], **Gunter Schumann**[10,28], **Hugh Garavan**[1,6,11], and **the IMAGEN Consortium**

[1]Department of Psychiatry, University of Vermont, Burlington, Vermont 05401, USA [2]Department of Psychology, University College Dublin, Dublin 4, Ireland [3]Department of Radiology, University of Vermont, Burlington, Vermont 05401, USA [4]Vermont Center for Children, Youth, and Families, University of Vermont, Burlington, Vermont 05401, USA [5]Department of Pediatrics, University of Vermont, Burlington, Vermont 05401, USA [6]Department of Psychology, University of Vermont, Burlington, Vermont 05401, USA [7]Institut National de la Santé et de la Recherche Médicale, INSERM CEA Unit 1000 “Imaging & Psychiatry”, University Paris Sud, 91400 Orsay, France [8]Department of Psychiatry, Orsay Hospital, 4 place du General Leclerc, 91400 Orsay, France [9]Department of Cognitive and Clinical Neuroscience, Central Institute of Mental Health, Medical Faculty Mannheim, Heidelberg University, 68159 Mannheim, Germany [10]Institute of Psychiatry, King’s College London, London SE5 8AF, UK [11]Institute of Neuroscience, Trinity College Dublin, Dublin 2, Ireland [12]Department of Systems Neuroscience, Universitätsklinikum Hamburg Eppendorf, 20246 Hamburg, Germany [13]Department of Psychology, Stanford University, Stanford, California 94305, USA [14]Department of Psychiatry, Université de Montreal, CHU Ste Justine Hospital, Montreal H3T 1C5, Canada [15]Department of Addictive Behaviour and Addiction Medicine, Heidelberg University, 68159 Mannheim, Germany [16]14 CEA, DSV, I2BM, Neurospin bat 145, 91191 Gif-Sur-Yvette, France [17]Department of Psychiatry and Psychotherapy, Campus Charité Mitte, Charité–Universitätsmedizin Berlin 10117, Germany [18]Department of Psychiatry and Neuroimaging Center, Technische Universität Dresden, 01062 Dresden, Germany [19]School of Physics and Astronomy, University of Nottingham, Nottingham NG7 2RD, UK [20]Physikalisch-

Correspondence and requests for materials should be addressed to R. Whelan (Robert.whelan@ucd.ie) or H.G. (Hugh.garavan@uvm.edu).

Supplementary Information is available in the online version of the paper.

Author Contributions T.B., G.J.B., A.L.W.B., C.B., F.M.C., P.J.C., H.F., M.F.-B., J.G., H.G., P.G., A.H., B.I., K.M., J.-L.M., F.N., T.P., M.R., C.L., Z.P., M.-L.P.-M., M.N.S., A.S., M.R. and T.W.R. acquired the data. R. Whelan., H.G., C.A.O. and N.O. analysed the behavioural data. G.G. calculated the family history data. R. Whelan, R. Watts and E.A. carried out neuroimaging data processing and analysis. R.R.A., V.F. and G.S. carried out genotyping and genetic analysis. R. Whelan and H.G. prepared the manuscript. C.A.O, P.J.C., J.G., T.P., T.W.R. and G.S. edited the manuscript.

The authors declare no competing financial interests.

Technische Bundesanstalt (PTB), 10587 Berlin, Germany [21]School of Psychology, University of Nottingham, Nottingham NG7 2RD, UK [22]AP-HP Department of Adolescent Psychopathology and Medicine, Maison de Solenn, University Paris Descartes, 75006 Paris, France [23]Neuroscience Graduate Program, University of Vermont, Burlington, Vermont 05401, USA [24]Rotman Research Institute, University of Toronto, Toronto, Ontario M5R 0A3, Canada [25]Montreal Neurological Institute, McGill University, H3A 2B4, Canada [26]The Hospital for Sick Children, University of Toronto, Toronto, OntarioM5G0A4, Canada [27]Behavioural and Clinical Neuroscience Institute and Department of Psychology, University of Cambridge, Cambridge CB2 1TN, UK [28]MRC Social, Genetic and Developmental Psychiatry (SGDP) Centre, London, London WC2R 2LS, UK

Abstract

A comprehensive account of the causes of alcohol misuse must accommodate individual differences in biology, psychology and environment, and must disentangle cause and effect. Animal models[1] can demonstrate the effects of neurotoxic substances; however, they provide limited insight into the psycho-social and higher cognitive factors involved in the initiation of substance use and progression to misuse. One can search for pre-existing risk factors by testing for endophenotypic biomarkers[2] in non-using relatives; however, these relatives may have personality or neural resilience factors that protect them from developing dependence[3]. A longitudinal study has potential to identify predictors of adolescent substance misuse, particularly if it can incorporate a wide range of potential causal factors, both proximal and distal, and their influence on numerous social, psychological and biological mechanisms[4]. Here we apply machine learning to a wide range of data from a large sample of adolescents (n = 692) to generate models of current and future adolescent alcohol misuse that incorporate brain structure and function, individual personality and cognitive differences, environmental factors (including gestational cigarette and alcohol exposure), life experiences, and candidate genes. These models were accurate and generalized to novel data, and point to life experiences, neurobiological differences and personality as important antecedents of binge drinking. By identifying the vulnerability factors underlying individual differences in alcohol misuse, these models shed light on the aetiology of alcohol misuse and suggest targets for prevention.

Alcohol misuse is common among adolescents[5]: slightly over 40% of all 13–14-year-old adolescents in the USA report alcohol use and 10% of this age group exhibit regular use. These figures rise to almost 65% for any alcohol use and 27%who report regular use by age 16 years. This is of concern as murine models demonstrate that adolescents are more vulnerable to alcohol-induced neurotoxicity than adults[1]. Early alcohol use is a strong risk factor for adult alcohol dependence[6] and therefore identifying inter-individual vulnerabilities and predictors of alcohol use inhuman adolescents is of importance. Generating such predictors, however, is challenging, not least because large sample sizes are needed to provide accurate estimates of the small effect sizes that prevail in the biological sciences[7,8]. Therefore, previous prospective studies, which typically focus on just one type of risk factor, have necessarily yielded modest predictions of future alcohol misuse. Moreover, previous classification approaches incorporating biological data have often been flawed due to overfitting[9,10,11].

Personality measures, particularly those assessing traits conferring risk for substance misuse, can identify adolescents at high risk of substance misuse[12].Life events in early adolescence, such as parental divorce[13], can also serve as predictors of future alcohol use. A number of candidate genes for alcohol dependence have been identified[14], although the overall risk conveyed by any one polymorphism is small[15]. Cognitive factors such as executive function (for example, inhibitory control), but not attention and visual memory, distinguished non-substance-using siblings of substance misusers from healthy controls[16]. Response inhibition was a modest predictor of adolescent alcohol misuse (explaining about 1% of variance) in a large sample of adolescents[17].Until now, there have been no large-sample prospective studies examining the neural correlates of alcohol misuse, but there is some evidence of a reduction in brain activity during tests of inhibitory control for adolescents who subsequently engaged in heavy alcohol use[18].

Here, we construct models of current and future adolescent binge drinking by combining a wide range of data (Extended Data Table 1) from the IMAGEN project[19,20], a multi-dimensional longitudinal study of adolescent development, using regularized logistic regression[21] (Extended Data Fig. 1). First (Analysis 1), we identified the characteristics discriminating 115 14-year-old binge drinkers (a minimum of three lifetime binge drinking episodes leading to drunkenness by age 14) from 150 14-year-old controls (non-binge drinkers, a maximum of two lifetime uses of alcohol until at least the age of 16; see Extended Data Table 2 for participant details) returning an area-under-the-curve (AUC) receiver-operator characteristic (ROC) value of 0.96 (95% CI = 0.93–0.98; see Extended Data Table 3a for all beta weights). At the optimum point in the ROC curve, 91% of binge drinkers and 91% of non-binge drinkers were correctly classified, significantly better than chance ($P = 8.0 \times 10^{-61}$). At the maximum *F*-score value, this classification accuracy corresponds to a precision rate of 87% (that is, those identified as binge drinkers who are actually binge drinkers) and a recall rate of 99% (that is, binge drinkers that are successfully detected; Extended Data Fig. 2a, b).

The model reported in Analysis 1, although highly accurate, was dominated by the inclusion of smoking, which often co-occurs with alcohol use. In Analysis 2, therefore, we removed smoking and re-ran the analyses (see Extended Data for all additional analyses with smoking included), which resulted in an AUC of 0.90 (95% CI = 0.86–0.93). At the optimum point in the ROC curve, 82% of binge drinkers and 89% of non-binge drinkers were correctly classified ($P = 8.8 \times 10^{-48}$). At the maximum *F*-score value the precision rate was 87% and the recall rate was 89% (Extended Data Fig. 2e, f). The features included in this model, and their strength of association with group membership, are displayed in Fig. 1a.

Figure 2a displays the brain regions that most consistently discriminated current binge drinkers from non-binge-drinkers (see Extended Data Fig. 3 for the contributions of each brain feature). The most robust brain classifiers were in ventromedial prefrontal cortex (vmPFC) and the left inferior frontal gyrus (IFG). The vmPFC grey matter volume was smaller in the current binge drinkers and this group, compared to controls, also showed decreased activity when anticipating or receiving a reward, but increased activity when processing angry faces. In the left IFG, current binge drinkers had smaller volumes and reduced activity when anticipating and receiving rewards and when processing angry faces.

The performance of each domain on its own (Analysis 3), both with and without age-14 smoking, is displayed in Extended Data Fig. 4a. The History and Personality domains were each accurate classifiers (AUC > 0.8).Next, we sought to quantify the unique contribution of each domain to the classification of current binge drinkers both with (Analysis 4) and without (Analysis 5) age-14smoking. To this end, we iteratively removed each domain from the full model (re-calculating the optimum elastic net parameters), and observed the relative reduction in classification accuracy (Extended Data Fig. 4b, c). The History domain contributed the greatest unique variance to the model (significant correlations among features are displayed in Extended Data Fig. 5). The results of external generalizations of the current binge drinking models with and without nicotine (Analyses 6 and 7, respectively) are displayed in Extended Data Fig. 2c, d, g, h.

We have described the profile of current alcohol misusers while also demonstrating the efficacy of our modelling approach. However, to identify risk factors for adolescent alcohol misuse, a matter of clinical relevance, a model that predicts future binge drinking is required. Thus, in Analysis 8, we compared 121 future binge drinkers (a maximum of two drink occasions by age 14 and a minimum of three lifetime binge drinking episodes by age 16) to the 150 controls described previously. This model had an AUC of 0.75 (95% CI = 0.69–0.80; Extended Data Fig. 2i, j). At the optimum point in the AUC curve, 73% of non-binge drinkers and 66% of binge drinkers were correctly classified, significantly better than chance ($P = 4.2 \times 10^{-17}$) given a base rate of 45% binge drinkers. This corresponds to a precision rate of 64% and a recall rate of 93% at the maximum *F*-score value. The features of the final model are displayed in Fig. 1b. Figure 2b displays the brain regions that discriminated future binge drinkers from non-binge-drinkers and the contributions of each functional/structural feature are displayed in Extended Data Fig. 6.

Next, we examined each domain on its own (Analysis 9). History was still the most predictive domain; however, now its influence was broadly comparable to Brain and Personality (Extended Data Fig. 4d), although the unique contribution of History was more apparent when each domain was iteratively removed from the model (Analysis 10; Extended Data Fig. 4e). Significant correlations among the features are displayed in Extended Data Fig. 7.

Our profile of adolescent binge drinking used a large sample and was internally valid, in that it generalized well using cross-validation. However, an outstanding question is whether or not this profile would be applicable to a new sample with different levels of alcohol consumption, which would speak to the dimensional nature of substance misuse[22]. Thus, we applied the prediction model from Analysis 8 to a new sample from the IMAGEN study (Analysis 11): all subjects had between 3–5 lifetime drink occasions (that is, a score of 2 on the substance misuse questionnaire) but no binge drinking episodes by age 14; by age 16, 61 of these still had no binge-drinking episodes whereas 55 participants had at least 3 binge-drinking episodes. Application of the model (without age-14 drinking as this was the same for all participants) resulted in similar predictability to that reported above: ROC AUC = 0.75 (95% CI = 0.66–0.83). At the optimal point of the AUC 77% of binge drinkers and 67% of non-binge-drinkers were correctly assigned ($P = 2.71 \times 10^{-8}$). At the maximum *F*-score value, this corresponds to a precision rate of 65% and a recall rate of 93%. The most

robust brain predictors of future binge drinking were the right middle and precentral gyri (Brodmann Area 6) and bilateral superior frontal gyrus (Brodmann Area 9). At age 14 future binge drinkers had reduced grey matter volume but increased activity when receiving a reward in the superior frontal gyrus compared to controls. In premotor cortex, future binge drinkers showed greater grey matter volume and greater activity when failing to inhibit.

A number of features were common to both current and future alcohol misuse (Analyses 2 and 8). Life events, such as a romantic or sexual relationship, were strong classifiers for both current and future binge drinkers. Personality measures associated with binge drinking included the novelty-seeking trait from the temperament and character inventory (TCI) psychobiological model of personality[23]. This trait identifies the behaviour of searching for, and feeling rewarded by, novel experiences and is regarded as a heritable, dopamine-related temperament: higher scores on Disorderliness and Extravagance (a tendency to approach reward cues) characterized both current and future binge drinkers. Conscientiousness (the degree to which an individual is organized, controlled and motivated to achieve a desired goal) was lower in both current and future binge drinkers.

Some features differed in their utility to classify current and future binge drinkers. Disruptive family events, the personality trait of agreeableness, more developed pubertal status, impulsivity and higher delay discounting (the tendency to devalue future rewards) classified current, but not future, binge drinkers. In contrast, the anxiety sensitivity subscale of the substance use risk profile scale (SURPS)[24] (fear of anxiety-related emotions and sensations due to beliefs that these emotions and sensations could lead to harmful consequences) predicted non-binge drinking at age 16, not at age 14. Parenchymal volume and grey:white matter ratio predicted future, but not current binge drinking. The most prominent brain regions for classifying current binge drinkers included the vmPFC and the left lateral PFC, areas that have been implicated in emotional regulation of bingeing behaviour[25,26]. Whereas emotional processing areas were implicated in age-14 binge drinking, predicting age-16 binge drinkers from data at age 14 relied relatively more on regions associated with failed inhibitory control and reward outcome and on local and global brain structure. Notably, even 1–2 lifetime alcohol occasions by age 14 was sufficient to be an important predictor of future binge drinking at age 16.

We have identified a generalizable risk profile for alcohol misuse initiation. In contrast with the classification of current binge drinkers, which was primarily a function of the History domain, the prediction of future binge drinking relied relatively more on a combination of three domains: History, Personality and Brain (individual ROC AUCs of 0.68, 0.67 and 0.63, respectively; Analysis 9). Thus, these results point to the value of a multi-domain analysis for predicting adolescent alcohol misuse and speak to the multiple causal factors for alcohol misuse. Further, we note that the influence of any one feature in isolation was modest, consistent with data showing that effect sizes in previous studies with smaller samples are likely to have been overestimated[7,9]. Given that the odds of adult alcohol dependence can be reduced by 10%for each year drinking onset is delayed in adolescence[27], this risk profile may facilitate the development of targeted interventions[24,28], which often yield higher effect sizes than general approaches[29].

METHODS

Overview of IMAGEN protocols

Full details of the procedures employed by the IMAGEN study, including details on ethics, recruitment, standardized instructions for administration of the psychometric and cognitive behavioural measures, and for blood collection and storage are available to view in the standard operating procedures for the IMAGEN project (http://www.imagen-europe.com/en/Publications_and_SOP.php). Informed consent was obtained from all subjects and their parents/guardians.

FMRI acquisition and analysis

Full details of the magnetic resonance imaging (MRI) acquisition protocols and quality checks have been described previously, including an extensive period of standardization across MRI scanners[19].

Functional MRI tasks

The stop signal task (SST), previously described in ref. 20 required volunteers to respond to regularly presented visual go stimuli (arrows pointing left or right) but to withhold their motor response when the go stimulus was followed unpredictably by a stop-signal (an arrow pointing upwards).We calculated contrast images for successful inhibitions (‘stop success’) and unsuccessful inhibitions (‘stop fail’), both versus an implicit baseline. The monetary incentive delay (MID) task (adapted from a task described previously[30]) required participants to respond to a briefly presented target by pressing either a left-hand or right-hand button as quickly as possible to indicate whether the target appeared on the left or the right side of the monitor display. If the participants responded while the target was on the screen, they scored points but if they responded before the target appeared or after the offset of the target they received no points. A cue preceded the onset of each trial, reliably indicating the position of the target and the number of points awarded for a successful response. A triangle indicated no points (no win), a circle with one line 2 points (small win) and a circle with three lines 10 points (large win). We calculated contrast images for the anticipation period of large win minus no win, and the outcome period for large win minus no win. The emotional reactivity task involved passive viewing of video clips that displayed ambiguous (emotionally “neutral”) or angry face expressions or control (non-biological motion) stimuli[31]. Each trial consisted of short (2 to 5 s) black-and-white video clips depicting either a face in movement or a control stimulus. We calculated contrast images from angry faces minus ambiguous faces.

Personality measures

Broad dimensions of personality were assessed using the 60-item neuroticism-extraversion-openness five-factor inventory, which returns measures on the dimensions of Extraversion, Agreeableness, Conscientiousness, Neuroticism, and Openness to Experience as described in the five-factor model of personality[32]. The substance use risk profile scale (SURPS[33]) assesses personality traits that confer risk for substance misuse and psychopathology along four distinct and independent personality dimensions; anxiety sensitivity, hopelessness,

sensation seeking, and impulsivity. The novelty seeking scale of the temperament and character inventory-revised (TCI-R[34]), which is composed of four sub-scales: Exploratory Excitability, Impulsiveness, Extravagance and Disorderliness, was administered.

Cognition

Participants completed a version of the Wechsler intelligence scale for children WISC-IV[35], of which we included the following subscales. Perceptual Reasoning, Matrix Reasoning, Similarities and Vocabulary. The monetary-choice questionnaire (MCQ[36]) was administered to provide a measure of preference of immediate lower over delayed higher monetary rewards. Participants completed five CANTAB tests: the Affective Go/No-go task, the Pattern Recognition Memory task, the Spatial Working Memory Task, the Rapid Visual Information Processing task, and the Cambridge Guessing Task (CGT). Behavioural data from functional imaging tasks included the mean Go reaction time and the standard deviation of the Go reaction time from the Stop Signal Task (inhibitory control). Behavioural data from the monetary incentive delay (reward) task were as follows: the number of Big Win trials on which the target was not hit, the number of Big Win trials on which the target was hit, the number of Small Win trials on which the target was not hit, the number of Small Win trials on which the target was hit, the number of No Win trials on which the target was not hit, and the number of No Win trials on which the target was hit. After the Emotional Reactivity tasks scanning session, participants completed a recognition task in which they were presented with three of the faces previously presented in the scanning session and two novel faces. Behavioural data from this task included the number of targets and the number of foils correctly categorized. Participants were not informed before the scanning session about the subsequent recall task.

History

The life-events questionnaire (LEQ) is an adaptation of the stressful life-event questionnaire[37], which uses 39 items to measure the lifetime occurrence and the perceived desirability of stressful events covering the following domains: Family/Parents, Accident/Illness, Sexuality, Autonomy, Deviance, Relocation, and Distress. The life-events valence labels were as follows: very unhappy, unhappy, neutral, happy, very happy. The pregnancy and birth questionnaire (PBQ, adapted from ref. 38) was completed by each participant's parent or guardian and parental cigarette and alcohol use during pregnancy were recorded, then recoded as binary variables. Subjects were classified into one of three categories: family history negative (a score of 0), neither positive nor negative (a score of 1), and family history positive (a score of 2).

Demographics

The puberty development scale (PDS[39]) was used to assess the pubertal status of our adolescent sample. The socioeconomic status score was comprised of the sum of the following variables: Mother's Education Score, Father's Education Score, Family Stress Unemployment Score, Financial Difficulties Score, Home Inadequacy Score, Neighbourhood Score, Financial Crisis Score, Mother Employed Score, Father Employed Score.

Genetics

We included single nucleotide polymorphisms (SNPs) described in a recent review[14] of genome wide association studies of alcohol dependence. Of the 30 unique SNPs listed in this review, the IMAGEN sample contained 14 SNPS that passed quality control, did not have a low minor allele frequency (<5%) or a high genotyping failure rate (>5%), and were not highly correlated (>.98) with any other available SNP. In addition, we also included an additional SNP, *rs26907*, reported in ref. 40. Genetic data were available on 1,835 individuals.

Substance misuse measures

The European School Survey Project on Alcohol and Drugs (ESPAD[41]) was administered. The ESPAD category scores are as follows (Score/Lifetime occurrences): 0(0), 1(1–2), 2(3–5), 3 (6–9), 4(10–19), 5(20–39), 6(40 or more). The primary questions of interest were regarding lifetime alcohol use (On how many occasions (if any) have you had any alcoholic beverage to drink?) and lifetime drunken episodes (On how many occasions (if any) have you been drunk from drinking alcoholic beverages?).

Machine learning procedure

We aimed to classify subjects based on both imaging and non-imaging data. Imaging data are comprised of a large number of potential predictive variables (voxels), which results in a high likelihood of overfitting (that is, fitting to the unique structure of a particular sample, resulting in a model with high apparent predictive value but which generalizes poorly to unseen data)[9]. Additionally, the high ratio of imaging to non-imaging variables would lead to the non-imaging variables being overwhelmed in any direct analysis. We overcome these issues through a multistep procedure in which each imaging contrast produced a single summary statistic for each individual (derived by identifying regions from different, training data), and nested cross-validation for tuning the parameters of the model and final validation (see Extended Data Fig. 1 for a schematic). This procedure was conducted for all seven domains (that is, all variables from Brain, Personality, History, Cognition, Demographics, Genetics and Site were included), for each domain separately (to assess how well each domain performed in isolation), and for six of the seven domains (to assess the unique contribution of a domain to the model by quantifying the decrement in performance of the full model arising from the deletion of one domain).

We implemented tenfold cross-validation with three levels of nesting for tuning and validating our model. A model is generated based on $k - 1$ training groups, and then applied to the remaining independent testing group. To implement cross-validation, the data are split into k groups (here $k = 10$). Each group serves as the testing group once, resulting in k different models and predictions for every subject based on independent data. In our approach, we had three levels of nested cross-validation (denoted inner, middle, and outer). At the inner fold, which was used to optimize the imaging thresholds, 72.9% (90%of 81%) of the subjects were used for training, 8.1%(10%of 81%) for testing, generating 1,000 voxel-wise logistic regression models. At the middle fold, which was used to optimize the parameters of the regularization, 81% (90%of 90%) of the subjects were used for training, 9% (10%of 90%) for testing, generating 100 models (note: new voxel-wise regression

models were generated at this step). At the outer fold, which was used to validate the model) 90% of the subjects were used for training, 10% for testing, generating 10 models (note: new voxel-wise regression models were generated at this step).

Model performance was quantified using the area under the curve (AUC) of the receiver operating characteristic (ROC) curve, which compares sensitivity versus specificity at various discrimination thresholds. In essence, the AUC of the ROC curve quantifies the model's ability to correctly assign a participant to the binge drinking group.

Generation of summary brain data (inner fold). The aim of this step was to generate brain maps of regions that differed between groups. Each iteration of Step 1 (see Extended Data Fig. 1) used 81% of the total sample: 72.9% of the sample as training data, the remaining 8.1% as testing data. All brain data (that is, each functional task and grey matter volume) were combined within a single, voxel-wise, logistic regression model, implemented via MATLAB's glmfit function. Specifically, at each voxel, data from reward anticipation and reward outcome contrasts from the MID, from the stop success and stop fail trials from the SST, angry versus neutral faces from the Faces task and proportional GMV (that is, GMV at that voxel divided by total brain GMV) were included in a single logistic regression analysis on the training data. Structural data were down-sampled from 1.5 mm to the same resolution as functional data (that is, 3 mm).

At each voxel, the area under the curve (AUC) of the receiver-operating characteristic (ROC) curve was computed on the test data. Maps of the AUC at each voxel and the contributions (beta weights) of each imaging contrast to the model were calculated. Given recent concern over the appropriate statistical thresholds in both neuroimaging and science generally[8,42,43], we sought to empirically determine the optimum, generalizable threshold for voxel-wise classification accuracy. To this end, binary masks of classification accuracy were generated over a range of AUC thresholds (that is, minimum values of AUC from 0.56 to 0.75 in 0.01 increments) and a range of cluster extent thresholds (1, 4, 8, 12, 16, 20, 24 contiguous voxels) and were applied to the contrast images (the functional data and grey matter volume) of the novel, test data.

The binary masks from the inner fold test group, using the optimized parameters, were then used to generate a summary statistic. This summary statistic was calculated for each imaging contrast in each subject, with the weighting based on the AUC and the contribution (that is, beta value from the logistic regression) of each imaging feature at each voxel, averaged over the number of voxels in the thresholded AUC mask.

Optimization of elastic net parameters (middle fold). The optimal brain threshold parameters were determined by the median best AUC and median best cluster extent across each middle fold. That is, each of the 100 models in the middle fold had an AUC threshold and a cluster extent that resulted in the highest classification accuracy on a novel test set (for example, the highest ROC AUC for a particular model on a novel test set could have been generated with a voxel-wise threshold of AUC = 0.67 and a cluster extent of 12 voxels). We took the median of these 100 best parameter sets (AUC threshold and voxel extent) to be the optimal set of parameters. Aggregating across the middle, and not inner fold meant that the

optimized parameters were not separate from the middle fold training data. We deliberately used the median of the parameters across each middle fold in order to attenuate the effects of spuriously high AUCs, and we reasoned that the impact on overfitting in the middle fold was likely to be minimal. Note that the final, outer fold, results were determined by performance on an entirely separate test fold (that is, the optimized parameters were determined on separate training data).

Separate brain maps were generated for each nested cross validation fold (that is, 100 sets of maps for the middle fold). These summary values were then used in the classification procedure, implemented via a logistic regression (that is, a logit link function) with elastic net variable selection and regularization[21], in combination with psychometric and other data. Feature scaling was performed on continuous and ordinal data by a *z*-score transformation. Continuous data were Winsorized (replacing data ±3 s.d. from the mean with the value at 3 s.d. from the mean).

The elastic net has two key parameters: λ (the regularization coefficient) and α (representing the weight of lasso versus ridge optimization, with intermediate values representing elastic net optimization). Again, we used nested cross-validation at the middle-fold level to optimize the values of λ and α. On each fold, λ and α were each set to one of 21 values (that is, all 441 combinations of λ and α were tested).Matlab's lassoglm (which implements lasso, ridge regression or elastic net constraints) was used to calculate the optimal model using maximum likelihood estimation. The median of the α and λ parameters that yielded the highest AUC across the middle fold were then used as inputs to the outer loop training set.

Final validation (outer fold). In the outer fold, the optimized brain and elastic net parameters were used to train a model on 90% of the sample, which was then tested on the remaining 10% of the sample. Ninety-five percent confidence intervals were estimated via 10,000 bootstraps.

External validation

In order to generate a single value for each brain metric for the external validation group (that is, each of the ten main folds had slightly different brain maps), we applied each of the maps from the outer loop data to the participants comprising the external validation (Analyses 6, 7 and 11). Next, we calculated the mean value across the 10 folds for each participant in the external validation group. Non-brain data were imputed in the same manner as the internal group. The median λ and α thresholds across all 10 folds of the internal sample (that is, the median of the median of the best λ and α values) were used as parameters for the elastic net.

Extended Data

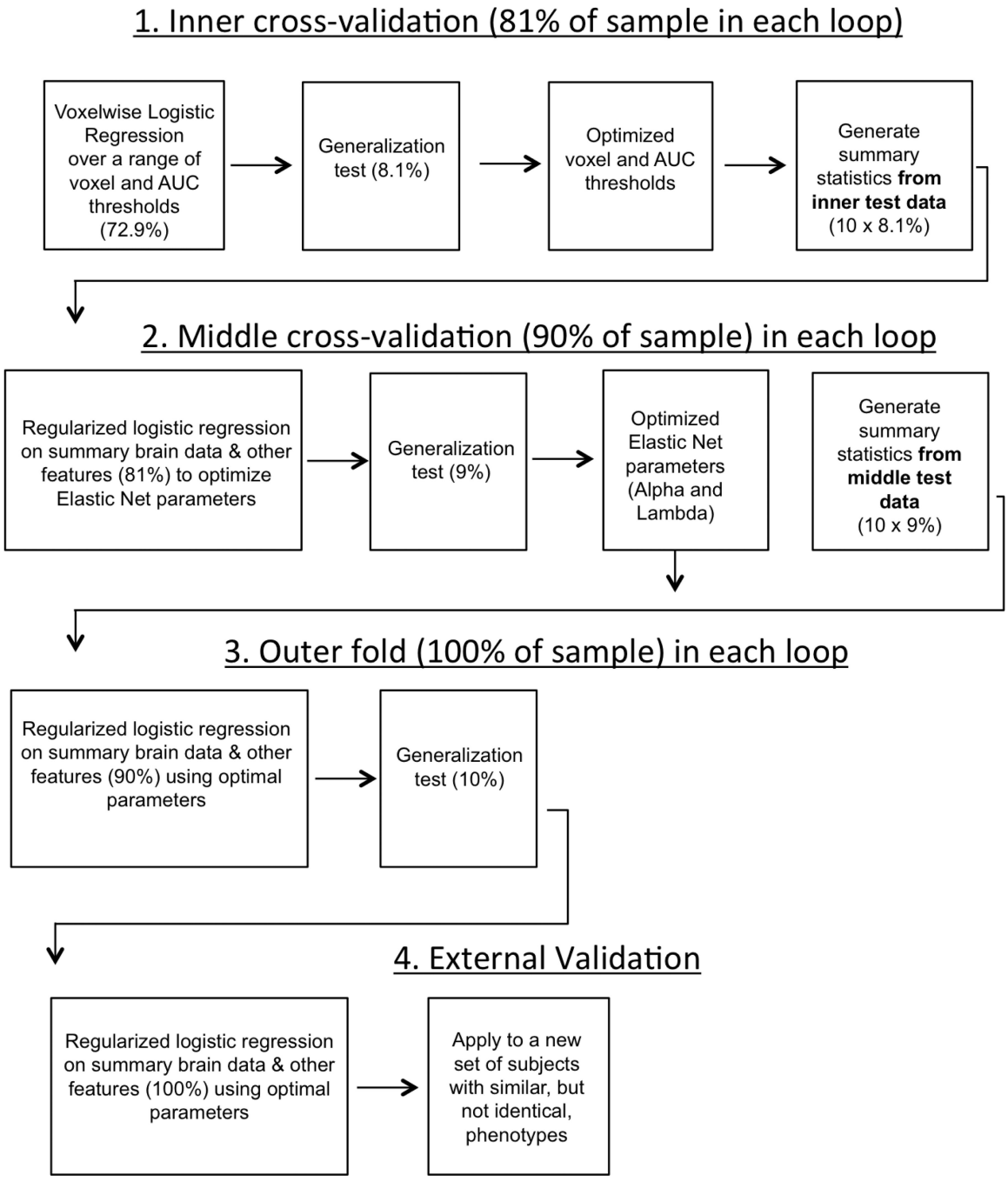

Extended Data Figure 1. A schematic of the analysis protocol

A schematic of the analysis protocol showing the inner cross-validation loop (to optimize the imaging parameters), the middle cross-validation loop (to optimize the elastic net parameters) and the outer loop (to quantify the generalizability). An external validation was also performed to quantify generalizability to a slightly different phenotype. The percentage of the sample used in each step is also displayed. AUC, area under the receiver-operating characteristic curve.

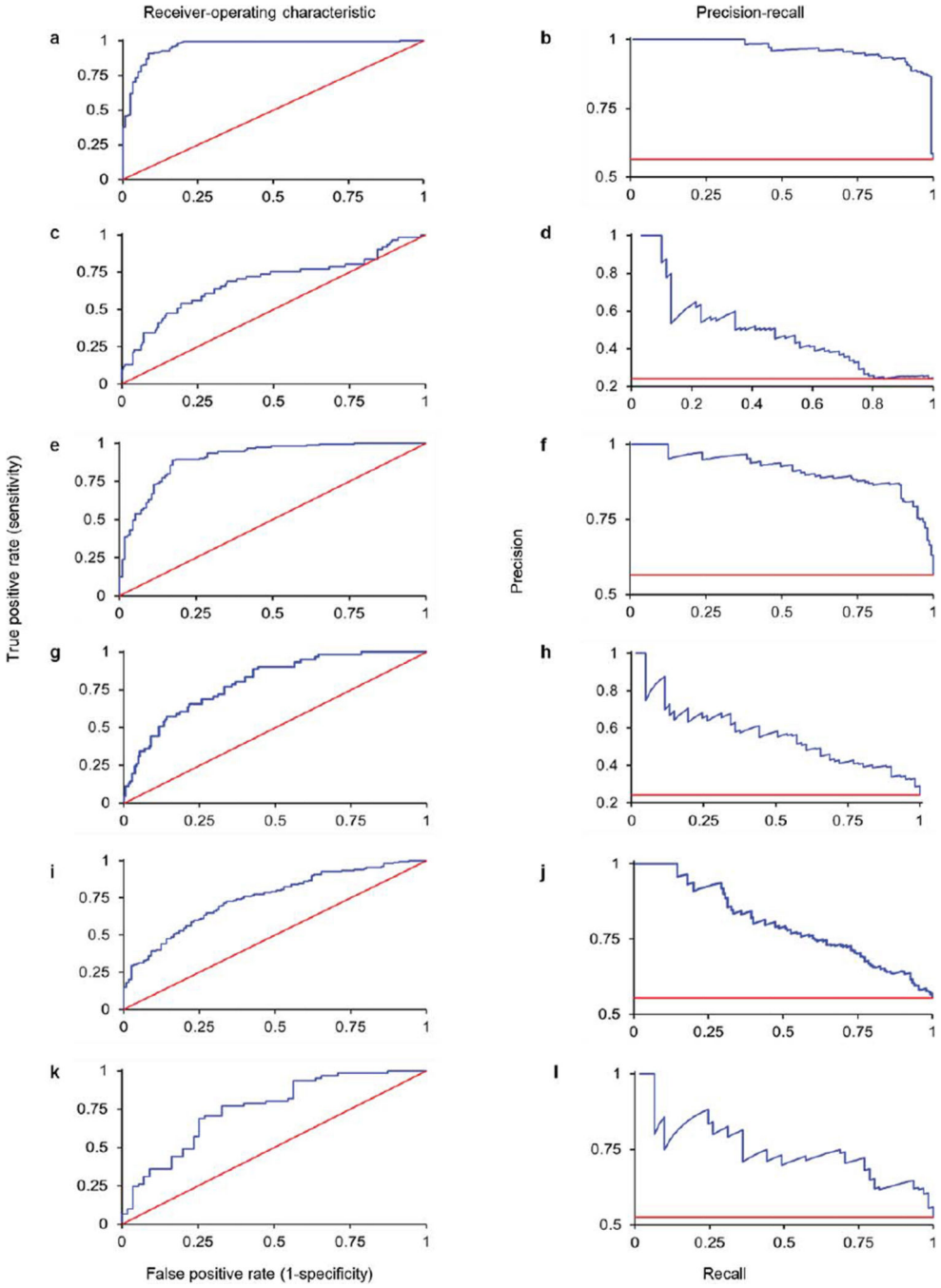

Extended Data Figure 2. Receiver-operating characteristics (ROC), precision-recall (PR) curves

a, ROC of age-14 binge drinking classification, with age-14 nicotine included (Analysis 1). **b**, PR of age-14 binge drinking classification, with age-14 nicotine included (Analysis 1). **c**, ROC of age-14 binge drinking external generalization, with age-14 nicotine included (Analysis 6). AUC = 0.68, 95% CI = 0.59–0.76). At the optimum point in the AUC curve, 93% of binge drinkers and 34% of non-binge drinkers were correctly classified, significantly better than chance (P = 0.035), given a base rate of 24% non-binge drinkers. **d**, PR of age-14 binge drinking external generalization, with age-14 nicotine included (Analysis 6). At the

maximum *F*-score value, this corresponds to a precision rate of 47% and a recall rate of 54%. **e**, ROC of age-14 binge drinking classification, with age-14 nicotine excluded (Analysis 2). **f**, PR of age-14 binge drinking classification, with age-14 nicotine excluded (Analysis 2). **g**, ROC of age-14 binge drinking external generalization, with age-14 nicotine excluded (Analysis 7). AUC = 0.80, 95% CI 0.73–0.85. At the optimum point in the AUC curve, 95% of binge drinkers and 34% of non-binge drinkers were correctly classified, significantly better than chance ($P = 0.016$), given a base rate of 24% non-binge drinkers. **h**, PR of age-14 binge drinking external generalization, with age-14 nicotine excluded (Analysis 7). At the maximum*F*-score value, this corresponds to a precision rate of 56% and a recall rate of 57%. **i**, ROC of age-16 binge drinking classification (Analysis 8). **j**, PR of age-16 binge drinking classification (Analysis 8). **k**, ROC of age-14 binge drinking external generalization (Analysis 11). **l**, PR of 14-year-old binge drinking external generalization (Analysis 11). AUC, area under the curve. CI, confidence interval.

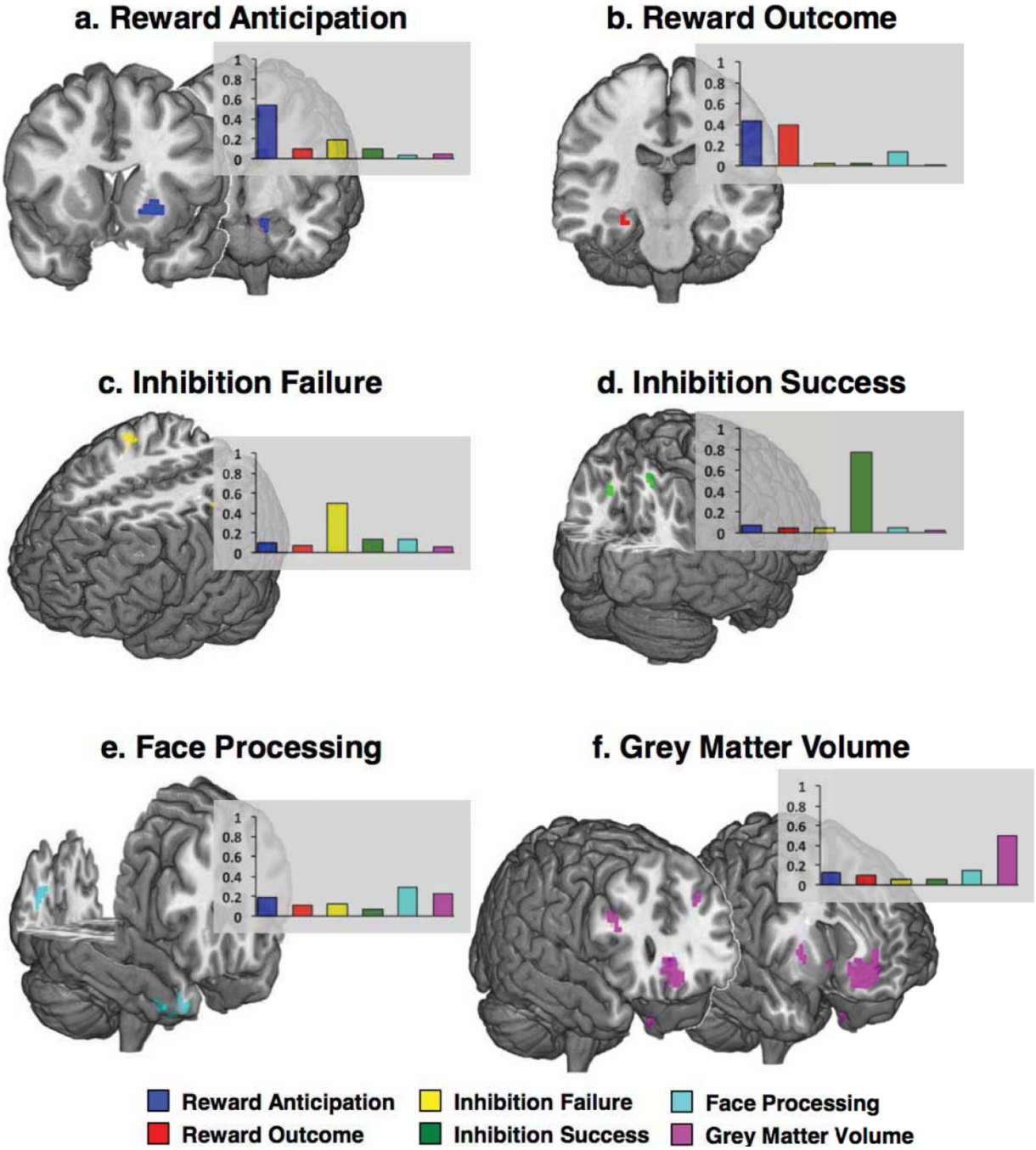

Extended Data Figure 3. Brain images showing regions that classify binge drinkers at age 14

The bar charts show the contribution of each brain metric to the shown clusters. The bar is the average beta weight for each brain metric (normalized to sum to 1 and averaged over the ten outer folds). **a, b**, Binge drinkers had reduced activity levels in the left putamen and left hippocampus when anticipating a reward (**a**) and reduced activity in the right hippocampus when rewards were received (**b**). **c–e**, Binge drinkers had greater activity in the right precentral and left postcentral gyri (**c**) when failing to inhibit a response and had greater activity in left and right precuneus (**d**) when they were successful in inhibiting. When

processing angry faces, binge drinkers showed reduced right temporal pole and right cuneus activity (**e**). **f**, Binge drinkers had reduced grey matter volume in bilateral ventromedial prefrontal cortex, right inferior and left middle frontal gyri, but increased volume in the right putamen.

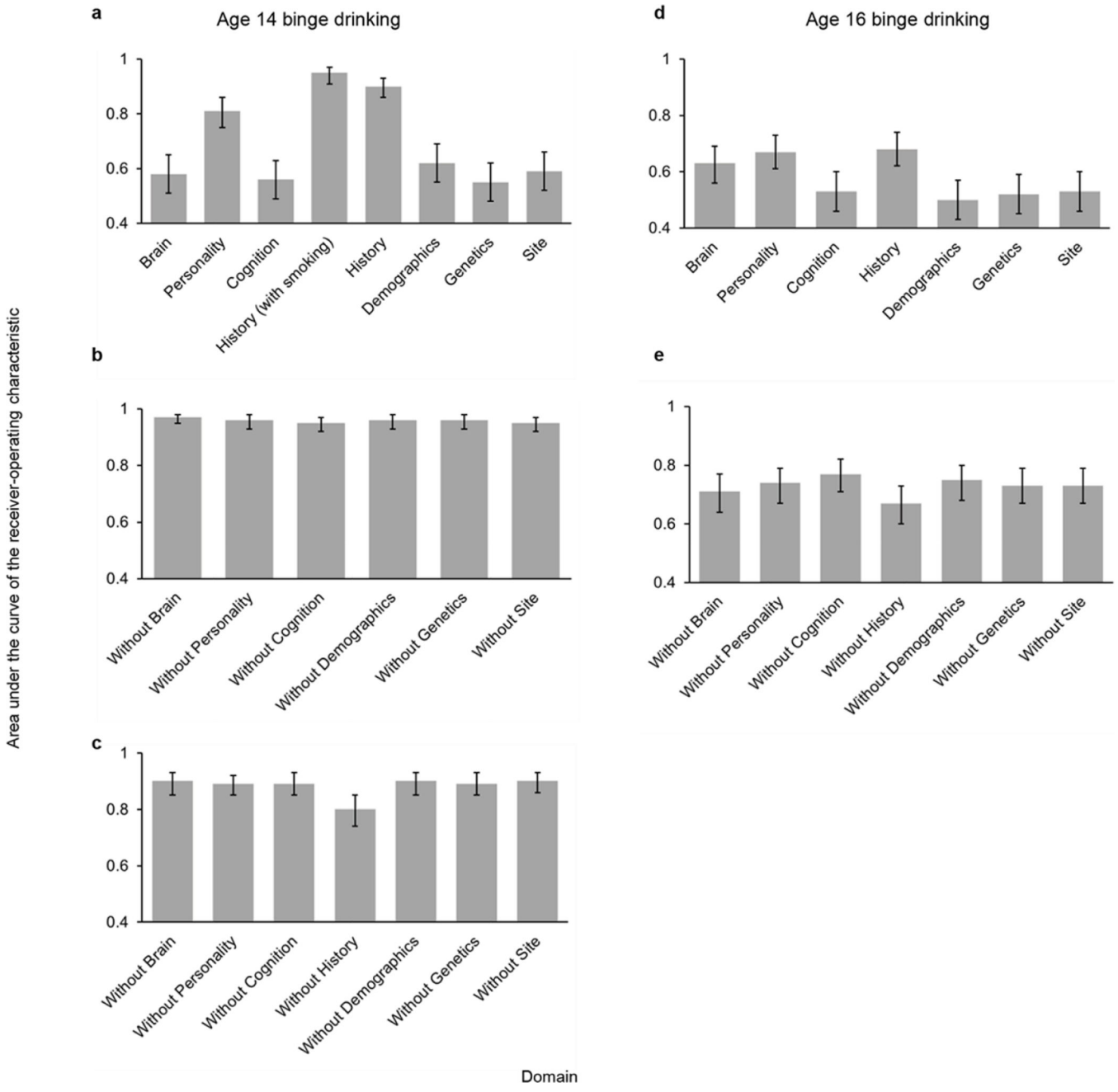

Extended Data Figure 4. Classification accuracy for each individual domain and the effects of removing each domain on the classification accuracy

The *y*-axis represents the area under the receiver-operating characteristic curve and the error bars represent the 95% confidence intervals (calculated via 10,000 bootstraps). **a**, The classification accuracy of age-14 binge drinking for each domain separately (Analysis 3). **b**,

the effects of removing each domain on the classification accuracy of age-14 binge drinking (nicotine included in the model; Analysis 4). **c**, the effects of removing each domain on the classification accuracy of age-14 binge drinking (nicotine excluded from the model; Analysis 5). **d**, The classification accuracy of age-16 binge drinking for each domain separately (Analysis 9). **e**, the effects of removing each domain on the classification accuracy of age-16 binge drinking (Analysis 10).

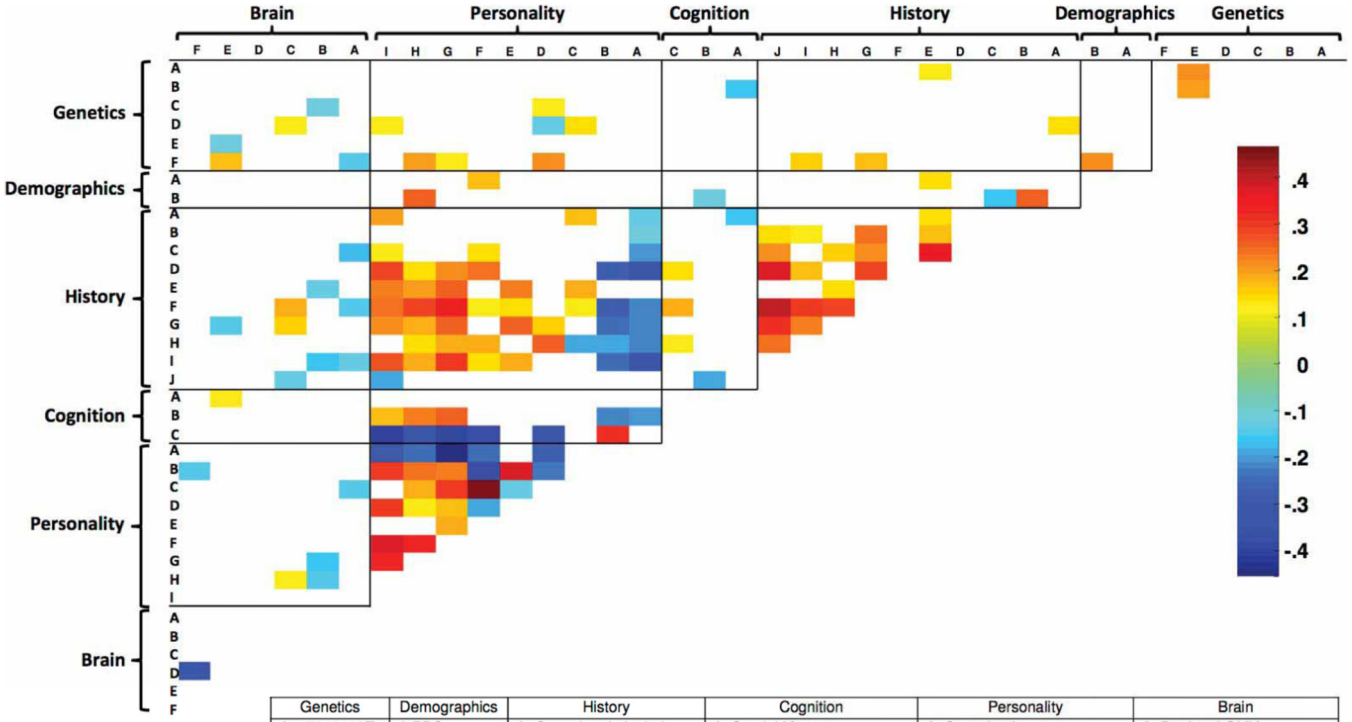

Genetics	Demographics	History	Cognition	Personality	Brain
A.rs7916403T	A.PDS	A. Gestational alcohol	A. Spatial Memory	A. Conscientiousness	A. Regional GMV
B.rs7590720G	B. Age	B. Family hx of drug Use	B. AGN Negative Target RT	B. Agreeableness	B. Emotional reactivity
C.rs7530302A		C. Romantic valence	C. Delay Discounting	C. Extraversion	C. Successful inhibition
D.rs2369955C		D. Family valence		D. Neuroticism	D. Inhibition failure
E.rs6701037C		E. Deviance valence		E. Sensation seeking	E. Reward outcome
F.rs2140418T		F. Autonomy valence		F. Hopelessness	F. Reward anticipation
		G. Romantic history		G. SURPS Impulsivity	
		H. Family history		H. Extravagance	
		I. Distress history		I. Disorganization	
		J. Deviance history			

Extended Data Figure 5. Correlations among the features classifying age-14 binge drinking

Significant correlations among the selected features (Analysis 2) are displayed (Spearman non-parametric test; $P < 0.05$). The colour bar denotes the correlation coefficient. GMV, grey matter volume; WMV, white matter volume; SWM, spatial working memory; AGN, affective go/no go; hx, history.

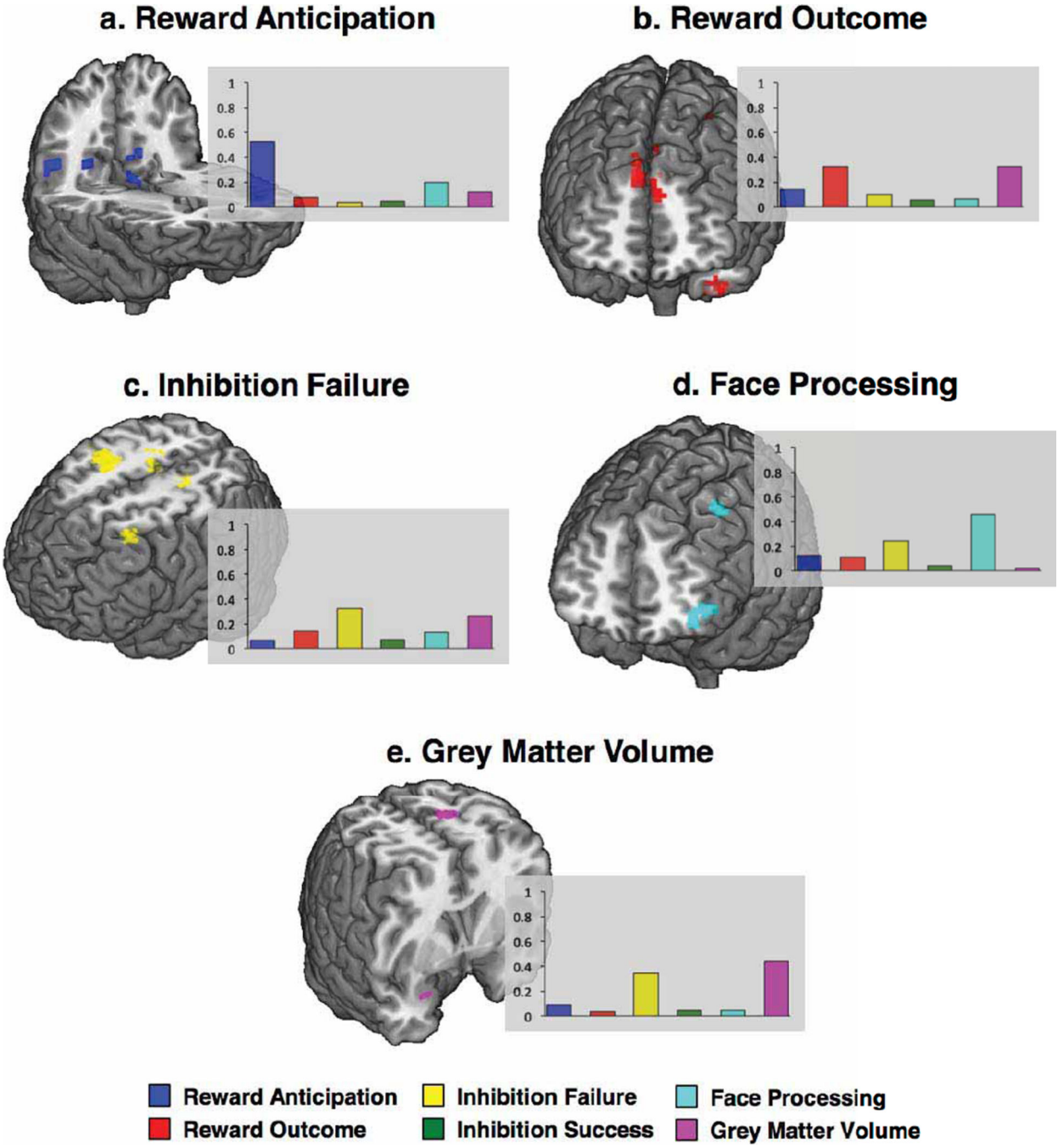

Extended Data Figure 6. The brain images show regions that predict binge drinking at age 16 from data collected at age 14

The bar charts show the contribution of each brain metric to the prediction accuracy of the shown clusters, which were derived from the training data. **a, b**, Future binge drinkers had reduced activation during reward anticipation in occipito-temporal and posterior cingulate regions (**a**) and for reward outcomes had reduced activity in the left temporal pole but increased activity in bilateral superior frontal gyrus (**b**). **c**, When failing to inhibit a motor response, future binge drinkers showed greater activity in the right middle, medial and

precentral gyri and in the left postcentral and middle frontal gyri. **d, e**, Future binge drinkers showed reduced activity in the left middle frontal gyrus when processing angry faces (**d**) and also had reduced grey matter volume in the right parahippocampal gyrus but increased grey matter volumes in the left postcentral gyrus (**e**).

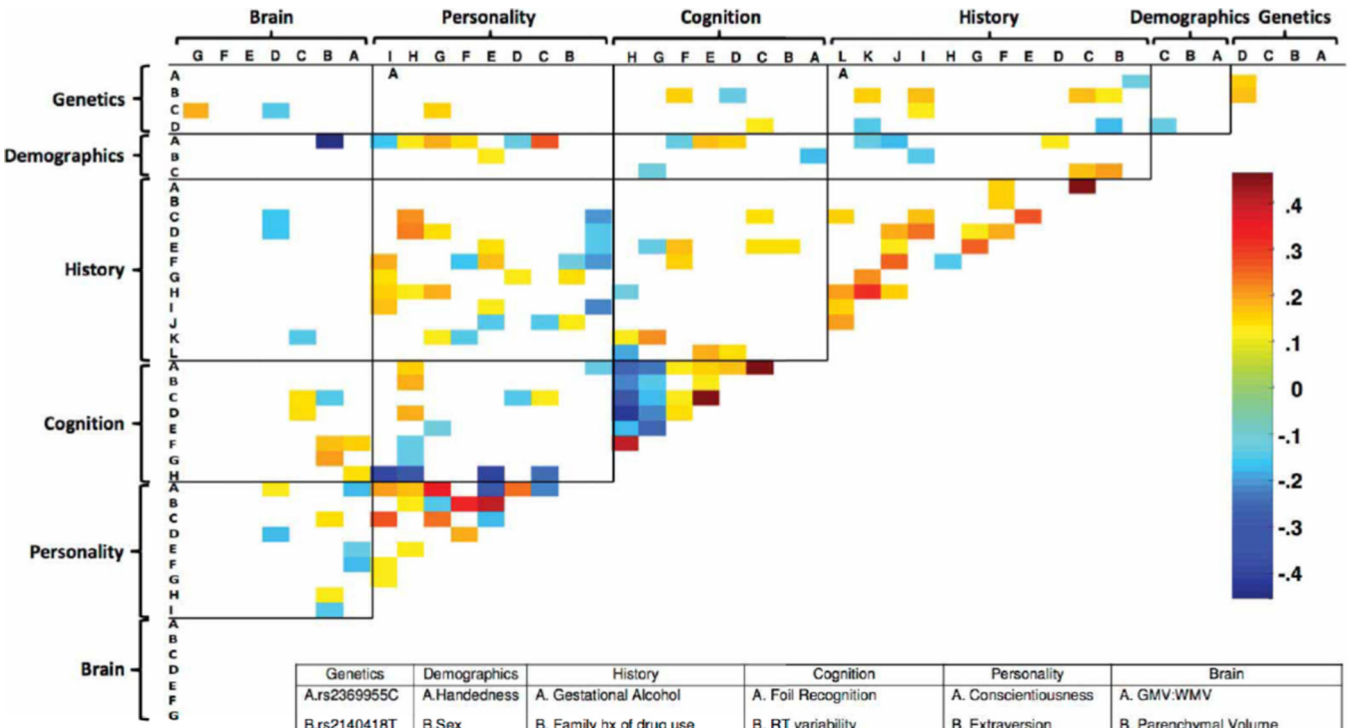

Genetics	Demographics	History	Cognition	Personality	Brain
A.rs2369955C	A.Handedness	A. Gestational Alcohol	A. Foil Recognition	A. Conscientiousness	A. GMV:WMV
B.rs2140418T	B.Sex	B. Family hx of drug use	B. RT variability	B. Extraversion	B. Parenchymal Volume
C.rs10893366T	C.Age	C. Family hx of alcohol use	C. RT mean	C. Neuroticism	C. Regional GMV
D.rs10758821T		D. 1-2 alcohol uses by age 14	D. SWM strategy	D. Sensation seeking	D. Emotional reactivity
		E. Smoking	E. SWM Errors	E. Hopelessness	E. Failed inhibition
		F. Family valence	F. AGN positive omissions	F. Anxiety sensitivity	F. Reward outcome
		G. Deviance valence	G. Verbal IQ	G. Excitability	G. Reward anticipation
		H. Autonomy valence	H. Performance IQ	H. Extravagance	
		I. Romantic history		I. Disorganization	
		J. Deviance history			
		K. Autonomy history			
		L. Accident history			

Extended Data Figure 7. Correlations among the features predicting age-16 binge drinking

Significant correlations among the selected features are displayed (Spearman non-parametric test; $P < 0.05$). The colour bar denotes the correlation coefficient. GMV, grey matter volume; WMV, white matter volume; SWM, spatial working memory; AGN, affective go/no go; hx, history.

Extended Data Table 1

A list of all features that were used

Domain	Measures	Features
Brain	Functional MRI: Monetary Incentive Delay task	Reward anticipation, reward outcome
	Functional MRI: Stop Signal Task	Inhibitory control success, Inhibitory control failure
	Functional MRI: Faces Task	Emotional reactivity to angry faces
	Structural MRI	Regional brain volume, parenchymal volume, grey-white matter ratio
Personality	Revised NEO Personality Inventory: Five-factor model	Neuroticism, openness, extraversion, agreeableness, conscientiousness
	Substance use risk profile scale	Anxiety sensitivity, impulsivity, negative thinking, sensation seeking
	Trait and character inventory: revised (novelty-seeking subscale)	Impulsivity, disorganization, extravagance, excitability
Cognition	Kirby	K: rate of delay discounting
	Wechsler Intelligence Scale for Children	Performance IQ, verbal IQ,
	Affective go/no-go	Negative target word reaction time, positive target word reaction time, negative target word omissions, positive target word omissions
	Cambridge Guessing Task	Delay aversion, deliberation time, decision quality, proportion bet (all trials), proportion bet (rational bets)
	CANTAB	Pattern recognition memory percentage correct, rapid visual processing d', spatial working memory errors, spatial working memory strategy
	Behavioural data: Monetary Incentive Delay task	Big reward (10 point) failures, big reward successes, small reward (5 point) failures, small reward successes, no reward failures, no reward successes
	Behavioural data: Stop Signal Task	All Go trials mean reaction time, all Go trials standard deviation reaction time
	Behavioural data: Faces Task	Face task target recognition, Face task foil recognition
History	Life events questionnaire (Frequency)	Accident, autonomy, deviance, distress, family relocation, romantic
	Life events questionnaire (Valence, perceived desirability)	Accident, autonomy, deviance, distress, family relocation, romantic
	European School Survey Project on Alcohol and Other Drugs	Age-14 smoking*, 1–2 alcohol occasions by 14†
	Family History questionnaire (general), diagnostic Michigan Alcohol Screening Test	Family history of alcohol misuse, drug misuse
	Pregnancy and Birth Questionnaire	Gestational exposure to cigarettes, alcohol
Demographics		Age, sex, pubertal development status, handedness, socioeconomic status
Site	Data acquisition center	London, Nottingham, Dublin, Mannheim, Berlin, Hamburg, Paris, Dresden
Genetics	Single nucleotide polymorphisms	rs10511260G, rs10758821T, rs10893366T, rs10975990G, rs1789891A, rs2140418T, rs6701037C, rs717207T, rs2369955C, rs26907A,

Domain	Measures	Features
		rs750338G, rs7530302A, rs7590720G, rs770182G, rs7916403T

Features are grouped by domain, by measure (for example, psychometric measure, functional imaging task, cognitive task) and by feature.

*Not included in all analyses.

†Not included in the analysis of age-14 drinking.

Extended Data Table 2

Subject characteristics and percentage of imputed data for each group

	Controls	Current Binge drinkers	Future binge drinkers	External validation controls	External validation current binge drinkers	External validation future binge drinkers
Group size	150	115	121	61	190	55
Analyses	1–5, 8–10	1–5	8–10	6,7,11	6,7	11
			Summary statistics			
Age (M/SD)	14.53(.43)	14.62(.39)	14.45 (0.40)	14.60(.37)	14.63(.44)	14.51(.49)
Sex (% female)	53	57	43	60	53	46
Lifetime drinks 14 (M/SD)	.29(.46)	4.23(1.39)	.59(.49)	2(0)	3.11(1.45)	2(0)
Lifetime drinks 16 (M/SD)	.54(.50)	5.22(1.22)	4.80(1.05)	3.18(1.39)	4.63(1.39)	4.74(1.01))
Cannabis 14 (M/SD)	.01(.08)	.69(1.49)	.03(.22)	0(0)	.26(.90)	.02(.13)
Cannabis 16 (M/SD)	.05(.50)	2.31(2.4)	1.39(1.8)	.10(.65)	1.33(1.96)	1.07(1.85)
Pubertal development scale (median/IQR)	4(1)	4(0)	4(1)	4(1)	4(1)	4(1)
Performance IQ (M/SD)	106(15)	105(16)	109(15)	114(14)	107(13)	111(14)
Verbal IQ (M/SD)	110(15)	108(14)	112(15)	113(14)	110(15)	116(13)
Socioeconomic status† (M/SD)	17.8(3.9)	17.1(4.0)	17.8(3.7)	18.8(3.7)	17.58(4.3)	17.8(3.6)
			% imputed data			
Pubertal development status	0.00	0.87	0.00	0.00	0.00	0.53
Substance use risk profile scale	0.66	4.35	0.83	0.00	0.00	2.11
Handedness	0.66	4.35	2.48	1.64	0.00	1.05
Trait and character inventory	0.00	1.74	0.00	0.00	0.00	1.05
Five-factor model	0.66	4.35	2.48	0.00	1.82	0.53
Wechsler Intelligence Scale	6.62	13.04	3.31	9.84	1.82	11.58
Temporal discounting	0.00	1.74	0.00	0.00	0.00	0.00
Life events questionnaire	5.96	5.22	1.65	3.28	3.64	2.11
Family history	1.32	1.74	1.65	0.00	1.82	0.00
CANTAB	1.99	6.09	2.48	3.28	3.64	1.05
Average imputed data	1.79	4.35	1.49	1.80	1.27	2.00

Summary statistics derived only from non-imputed data. The external validation current binge drinker group consisted of 190 new subjects from the IMAGEN sample with 1–2 binge-drinking episodes by age 14.

M, mean; SD, standard deviation; IQR, interquartile range.

Extended Data Table 3

Beta weights for classification of age-14 binge drinking and prediction of age-16 binge drinking

a

Feature	Mean Beta	SEM
Constant	0.232	0.053
Reward anticipation	0.208	0.051
Reward outcome	0.359	0.039
Emotional reactivity	0.270	0.033
Regional GMV	0.204	0.019
Extravagance	−0.210	0.018
SURPS impulsivity	−0.077	0.017
Hopelessness	−0.102	0.015
Sensation seeking	−0.181	0.029
Deviance history	−0.191	0.018
Distress history	−0.109	0.015
Family history	−0.229	0.026
Romantic history	−0.547	0.060
Autonomy valence	−0.313	0.041
Deviance valence	−0.174	0.026
Family hx drug misuse	−0.141	0.017
Smoking	−1.681	0.259
Pubertal Development Status	−0.061	0.012
Site 2	−0.346	0.043

b

Feature	Mean Beta	SEM
Constant	0.356	0.012
Reward anticipation	0.076	0.008
Reward outcome	0.109	0.013
Failed inhibition	0.085	0.015
Successful inhibition	0.087	0.011
Emotional reactivity	0.127	0.009
Regional GMV	0.110	0.012
Disorganization	−0.067	0.007
Extravagance	−0.124	0.013
SURPS impulsivity	−0.065	0.004
Hopelessness	−0.054	0.005
Sensation seeking	−0.077	0.009
Neuroticism	−0.039	0.005
Extraversion	−0.044	0.004
Agreeableness	0.065	0.004

b

Feature	Mean Beta	SEM
Conscientiousness	0.071	0.007
Delay discounting	−0.051	0.004
AGN negative targets RT	0.039	0.005
SWM errors	0.053	0.007
Deviance history	−0.178	0.018
Distress history	−0.092	0.009
Family history	−0.140	0.015
Romantic history	−0.244	0.029
Autonomy valence	−0.071	0.010
Deviance valence	−0.172	0.021
Family valence	−0.055	0.006
Romantic valence	−0.022	0.003
Family hx drug misuse	−0.048	0.009
Gestational alcohol	−0.040	0.006
Age	−0.016	0.003
Pubertal Development Status	−0.090	0.010
Site 2	−0.086	0.011
Site 3	0.039	0.005
rs2140418T	−0.027	0.004
rs6701037C	−0.051	0.007
rs2369955C	−0.030	0.005
rs7530302A	−0.018	0.004
rs7590720G	−0.030	0.004
rs7916403T	−0.065	0.009

c

Feature	Mean Beta	SEM
Constant	0.259	0.011
Reward anticipation	0.115	0.024
Reward outcome	0.225	0.021
Failed inhibition	0.177	0.027
Emotional reactivity	0.136	0.020
Regional GMV	0.164	0.014
Parenchymal volume	−0.102	0.013
GMV:WMV	0.071	0.007
Disorganization	−0.025	0.005
Extravagance	−0.082	0.011
Excitability	−0.083	0.011
Anxiety sensitivity	0.075	0.013
Hopelessness	−0.076	0.013
Sensation seeking	−0.054	0.007

c

Feature	Mean Beta	SEM
Neuroticism	−0.027	0.009
Extraversion	−0.062	0.010
Conscientiousness	0.086	0.008
Performance IQ	−0.051	0.007
Verbal IQ	−0.042	0.007
AGN positive omissions	0.040	0.007
SWM errors	0.066	0.008
SWM strategy	0.065	0.011
RT mean	−0.022	0.004
RT variability	−0.081	0.012
Foil recognition	0.106	0.017
Accident history	−0.051	0.007
Autonomy history	−0.039	0.007
Deviance history	−0.078	0.009
Romantic history	−0.184	0.023
Autonomy valence	−0.040	0.010
Deviance valence	−0.134	0.015
Family valence	−0.077	0.014
Smoking	−0.052	0.007
1–2 alcohol occasions by 14	−0.180	0.020
Family hx alcohol misuse	−0.024	0.006
Family hx drug misuse	−0.054	0.011
Gestational alcohol	−0.066	0.013
Age	0.046	0.010
Sex	0.033	0.005
Handedness	−0.062	0.010
Site 1	0.035	0.005
Site 5	−0.095	0.012
Silt 7	0.038	0.006
rs10758821T	−0.028	0.005
rs10893366T	0.028	0.008
rs2140418T	−0.040	0.007
rs2369955C	−0.067	0.010

a, Mean beta weights (averaged over 10 outer folds) and the standard error of the mean (SEM) beta for classification of age-14 binge drinking (Analysis 1). **b**, Mean and SEM of the beta weights for classification of age-14 binge drinking (Analysis 2). **c**, Mean and SEM of the beta weights for prediction of age-16 binge drinking (Analysis 8).

Acknowledgements

This work received support from the following sources: the European Union-funded FP6 Integrated Project IMAGEN (Reinforcement-related behaviour in normal brain function and psychopathology) (LSHM-CT-2007-037286), the FP7 projects IMAGEMEND (602450; IMAging GEnetics for MENtal Disorders) and MATRICS (603016), the Innovative Medicine Initiative Project EU-AIMS (115300-2), a Medical Research Council Programme Grant “Developmental pathways into adolescent substance abuse” (93558), the Swedish funding agency FORMAS, the Medical Research Council and the Wellcome Trust (Behavioural and Clinical

Neuroscience Institute, University of Cambridge), the National Institute for Health Research (NIHR) Biomedical Research Centre at South London and Maudsley NHS Foundation Trust and King's College London, the Bundesministeriumfür Bildung und Forschung (BMBF grants 01GS08152; 01EV0711; eMED SysAlc01ZX1311A; Forschungsnetz AERIAL), the Deutsche Forschungsgemeinschaft (DFG): Reinhart-Koselleck Award SP 383/5-1 and grants SM 80/7-1, SFB 940/1, FOR 1617), the French MILDT (Mission Interministérielle de Lutte contre la Drogue et la Toxicomanie), the CENIR (Centre de NeuroImagerie de Recherche, Pr. S. Lehéricy) within the ICM institute, the National Institute of Mental Health(MH082116), a National Institutes of Health Center of Biomedical Research Excellence award P20GM103644 from the National Institute of General Medical Sciences and the Tobacco Centers of Regulatory Science award P50DA036114. The authors acknowledge the Vermont Advanced Computing Core which is supported by NASA (NNX 06AC88G), at the University of Vermont for providing high performance computing resources that have contributed to the research results reported within this paper.

The IMAGEN Consortium

Lisa Albrecht[1], Mercedes Arroyo[2], Semiha Aydin[3], Christine Bach[4], Alexis Barbot[5], Zuleima Bricaud[6], Uli Bromberg[7], Ruediger Bruehl[3], Anna Cattrell[8], Katharina Czech[1], Jeffrey Dalley[2], Sylvane Desrivieres[8], Tahmine Fadai[7], Birgit Fuchs[9], Fanny Gollier Briand[6], Kay Head[10], Bert Heinrichs[11], Nadja Heym[10], Thomas Hübner[12], Albrecht Ihlenfeld[3], James Ireland[13], Nikolay Ivanov[1], Tianye Jia[8], Jennifer Jones[14], Agnes Kepa[8], Dirk Lanzerath[11], Mark Lathrop[15], Hervé Lemaitre[6], Katharina Lüdemann[1], Lourdes Martinez-Medina[8], Xavier Mignon[16], Ruben Miranda[6], Kathrin Müller[12], Charlotte Nymberg[8], Jani Pentilla[6], Jean-Baptiste Poline[5], Luise Poustka[4], Michael Rapp[1], Stephan Ripke[12], Sarah Rodehacke[12], John Rogers[13], Alexander Romanowski[1], Barbara Ruggeri[8], Christine Schmäl[4], Dirk Schmidt[12], Sophia Schneider[7], Markus Schroeder[17], Florian Schubert[3], Wolfgang Sommer[4], Rainer Spanagel[4], David Stacey[8], Sabina Steiner[4], Dai Stephens[18], Nicole Strache[1], Maren Struve[4], Amir Tah masebi[19], Lauren Topper[8], Helene Vulser[6], Bernadeta Walaszek[3], Helen Werts[8], Steve Williams[8], C. Peng Wong[8], Juliana Yacubian[7] & Veronika Ziesch[12].

[1]Campus Charité Mitte, Charité–Universitätsmedizin, Berlin10117, Germany. [2]University of Cambridge, Cambridge CB2 1TN, UK. [3]Physikalisch-Technische Bundesanstalt (PTB), 10587 Berlin, Germany. [4]Central Institute of Mental Health, Medical Faculty Mannheim, Heidelberg University, 68159 Mannheim, Germany. [5]Commissariat à l'Energie Atomique, 14 CEA, DSV, I2BM, Neurospin bat 145, 91191 Gif-Sur-Yvette, France. [6]Institut National de la Santé et de la Recherche Médicale, INSERM CEA Unit 1000 "Imaging & Psychiatry", University Paris Sud, 91400 Orsay, France. [7]Universitätsklinikum Hamburg Eppendorf, 20246 Hamburg, Germany. [8]Institute of Psychiatry, King's College London, London SE5 8AF, UK. [9]GABO:milliarium mbH & Co. KG 80333 Munich, Germany. [10]University of Nottingham, Nottingham NG7 2RD, UK. [11]Deutsches Referenzzentrum für Ethik, D 53113 Bonn, Germany. [12]Technische Universität Dresden, 01062 Dresden, Germany. [13]Delosis, Twickenham, Middlesex TW1 4AE, UK. [14]Trinity College Dublin, Dublin 2, Ireland. [15]Centre National de Génotypage, 91057 Evry Cedex, France. [16]PERTIMM, 92600 Asnières-Sur-Seine, France. [17]Tembit Software GmbH, 13507 Berlin, Germany. [18]University of Sussex, Brighton BN1 9RH, UK. [19]University of Toronto, Toronto, Ontario M5G 0A4, Canada.

References

1. Crews FT, Braun CJ, Hoplight B, Switzer RC III, Knapp DJ. Binge ethanol consumption causes differential brain damage in young adolescent rats compared with adult rats. Alcohol. Clin. Exp. Res. 2000; 24:1712–1723. [PubMed: 11104119]
2. Ersche KD, et al. Abnormal brain structure implicated in stimulant drug addiction. Science. 2012; 335:601–604. [PubMed: 22301321]
3. Volkow ND, et al. High levels of dopamine D2receptors in unaffected members of alcoholic families: possible protective factors. Arch. Gen. Psychiatry. 2006; 63:999–1008. [PubMed: 16953002]
4. Cloninger CR. Neurogenetic adaptive mechanisms in alcoholism. Science. 1987; 236:410–416. [PubMed: 2882604]
5. Swendsen J, et al. Use and abuse of alcohol and illicit drugs in US adolescents: results of the National Comorbidity Survey-Adolescent Supplement. Arch. Gen. Psychiatry. 2012; 69:390–398. [PubMed: 22474107]
6. Grant JD, et al. Adolescent alcohol use is a risk factor for adult alcohol and drug dependence: evidence from a twin design. Psychol. Med. 2006; 36:109–118. [PubMed: 16194286]
7. Ioannidis JP. Why most published research findings are false. PLoS Med. 2005; 2:e124. [PubMed: 16060722]
8. Button KS, et al. Power failure: why small sample size undermines the reliability of neuroscience. Nature Rev. Neurosci. 2013; 14:365–376. [PubMed: 23571845]
9. Whelan R, Garavan H. Prediction inflation in neuroimaging. Biol. Psychiatry. 2014; 75:746–748. [PubMed: 23778288]
10. Bellazzi R, Zupan B. Predictive data mining in clinical medicine: current issues and guidelines. Int. J. Med. Inform. 2008; 77:81–97. [PubMed: 17188928]
11. Ambroise C, McLachlan G. Selection bias in gene extraction on the basis of microarray gene-expression data. Proc. Natl Acad. Sci. USA. 2002; 99:6562–6566. [PubMed: 11983868]
12. Castellanos-Ryan N, O'Leary-Barrett M, Sully L, Conrod P. Sensitivity and specificity of a brief personality screening instrument in predicting future substance use, emotional, and behavioral problems: 18-month predictive validity of the Substance Use Risk Profile Scale. Alcohol. Clin. Exp. Res. 2013; 37:E281–E290. [PubMed: 22974180]
13. Dube S, et al. Adverse childhood experiences and the association with ever using alcohol and initiating alcohol use during adolescence. J. Adolesc. Health. 2006; 38:444.e1–444.e10. [PubMed: 16549308]
14. Rietschel M, Treutlein J. The genetics of alcohol dependence. Ann. NY Acad. Sci. 2013; 1282:39–70. [PubMed: 23170934]
15. Tyndale RF. Genetics of alcohol and tobacco use in humans. Ann. Med. 2003; 39:94–121. [PubMed: 12795339]
16. Ersche KD, et al. Cognitive dysfunction and anxious-impulsive personality traits are endophenotypes for drug dependence. Am. J. Psychiatry. 2012; 169:926–936. [PubMed: 22952072]
17. Nigg J, et al. Poor response inhibition as a predictor of problem drinking and illicit drug use in adolescents at risk for alcoholism and other substance use disorders. J. Am. Acad. Child Adolesc. Psychiatry. 2006; 45:468–475. [PubMed: 16601652]
18. Norman AL, et al. Neural activation during inhibition predicts initiation of substance use in adolescence. Drug Alcohol Depend. 2011; 119:216–223. [PubMed: 21782354]
19. Schumann G, et al. The IMAGEN study: reinforcement-related behaviour in normal brain function and psychopathology. Mol. Psychiatry. 2010; 15:1128–1139. [PubMed: 21102431]
20. Whelan R, et al. Adolescent impulsivity phenotypes characterized by distinct brain networks. Nature Neurosci. 2012; 15:920–925. [PubMed: 22544311]
21. Zou H, Hastie T. Regularization and variable selection via the elastic net. J. Roy. Stat. Soc. B. 2005; 67:301–320.

22. Robbins TW, Gillan C, Smith D, de Wit S, Ersche K. Neurocognitive endophenotypes of impulsivity and compulsivity: towards dimensional psychiatry. Trends Cogn. Sci. 2012; 16:81–91. [PubMed: 22155014]
23. Cloninger CR, Svrakic DM, Przybeck TR. A psychobiological model of temperament and character. Arch. Gen. Psychiatry. 1993; 50:975–990. [PubMed: 8250684]
24. Conrod PJ, Castellanos N, Mackie C. Personality-targeted interventions delay the growth of adolescent drinking and binge drinking. J. Child Psychol. Psychiatry. 2008; 49:181–190. [PubMed: 18211277]
25. Goldstein RZ, Volkow N. Dysfunction of the prefrontal cortex in addiction: neuroimaging findings and clinical implications. Nature Rev. Neurosci. 2011; 12:652–669. [PubMed: 22011681]
26. Hare TA, Camerer CF, Rangel A. Self-control in decision-making involves modulation of the vmPFC valuation system. Science. 2009; 324:646–648. [PubMed: 19407204]
27. Grant BF, Stinson FS, Harford TC. Age at onset of alcohol use and DSM-IV alcohol abuse and dependence: a 12-year follow-up. J. Subst. Abuse. 2001; 13:493–504. [PubMed: 11775078]
28. Ghahremani DG, et al. Effects of the Youth Empowerment Seminar on impulsive behavior in adolescents. J. Adolesc. Health. 2013; 53:139–141. [PubMed: 23601502]
29. Gottfredson DC, Wilson DB. Characteristics of effective school-based substance abuse prevention. Prev. Sci. 2003; 4:27–38. [PubMed: 12611417]
30. Knutson B, Fong GW, Adams CM, Varner JL, Hommer D. Dissociation of reward anticipation and outcome with event-related fMRI. Neuroreport. 2001; 12:3683–3687. [PubMed: 11726774]
31. Grosbras M-H, Paus T. Brain networks involved in viewing angry hands or faces. Cereb. Cortex. 2006; 16:1087–1096. [PubMed: 16221928]
32. Costa PT, McCrae R. Domains and facets: hierarchical personality assessment using the revised NEO personality inventory. J. Pers. Assess. 1995; 64:21–50. [PubMed: 16367732]
33. Woicik PA, Stewart S, Pihl R, Conrod P. The Substance Use Risk Profile Scale: a scale measuring traits linked to reinforcement-specific substance use profiles. Addict. Behav. 2009; 34:1042–1055. [PubMed: 19683400]
34. Cloninger, CR. The Temperament and Character Inventory-Revised. Washington Univ.; 1999.
35. Wechsler, D. Wechsler Intelligence Scale For Children–Fourth Edition (WISC-IV). The Psychological Corporation; 2003.
36. Kirby KN, Petry NM, Bickel WK. Heroin addicts discount delayed rewards at higher rates than non-drug using controls. J. Exp. Psychol.Gen. 1999; 128:78–87. [PubMed: 10100392]
37. Newcomb MD, Huba GJ, Bentler PM. A multidimensional assessment of stressful life events among adolescents: derivation and correlates. J. Health Soc. Behav. 1981; 22:400–415.
38. Pausova Z, et al. Genes, maternal smoking, and the offspring brain and body during adolescence: design of the Saguenay Youth Study. Hum. Brain Mapp. 2007; 28:502–518. [PubMed: 17469173]
39. Petersen AC, Crockett L, Richards M. A self-report measure of pubertal status: reliability, validity, and initial norms. J. Youth Adolesc. 1988; 17:117–133. [PubMed: 24277579]
40. Stacey D, et al. *RASGRF2* regulates alcohol-induced reinforcement by influencing mesolimbic dopamine neuron activity and dopamine release. Proc. Natl Acad. Sci. USA. 2012; 109:21128–21133. [PubMed: 23223532]
41. Hibell B, et al. The 1995 ESPAD report: alcohol and other drug use among students in 26 European countries. Swedish Council for Information on Alcohol and Other Drugs. 1997
42. Johnson VE. Revised standards for statistical evidence. Proc. Natl Acad. Sci. USA. 2013; 110:19313–19317. [PubMed: 24218581]
43. Nuzzo R. Scientific method: statistical errors. Nature. 2014; 506:150–152. [PubMed: 24522584]

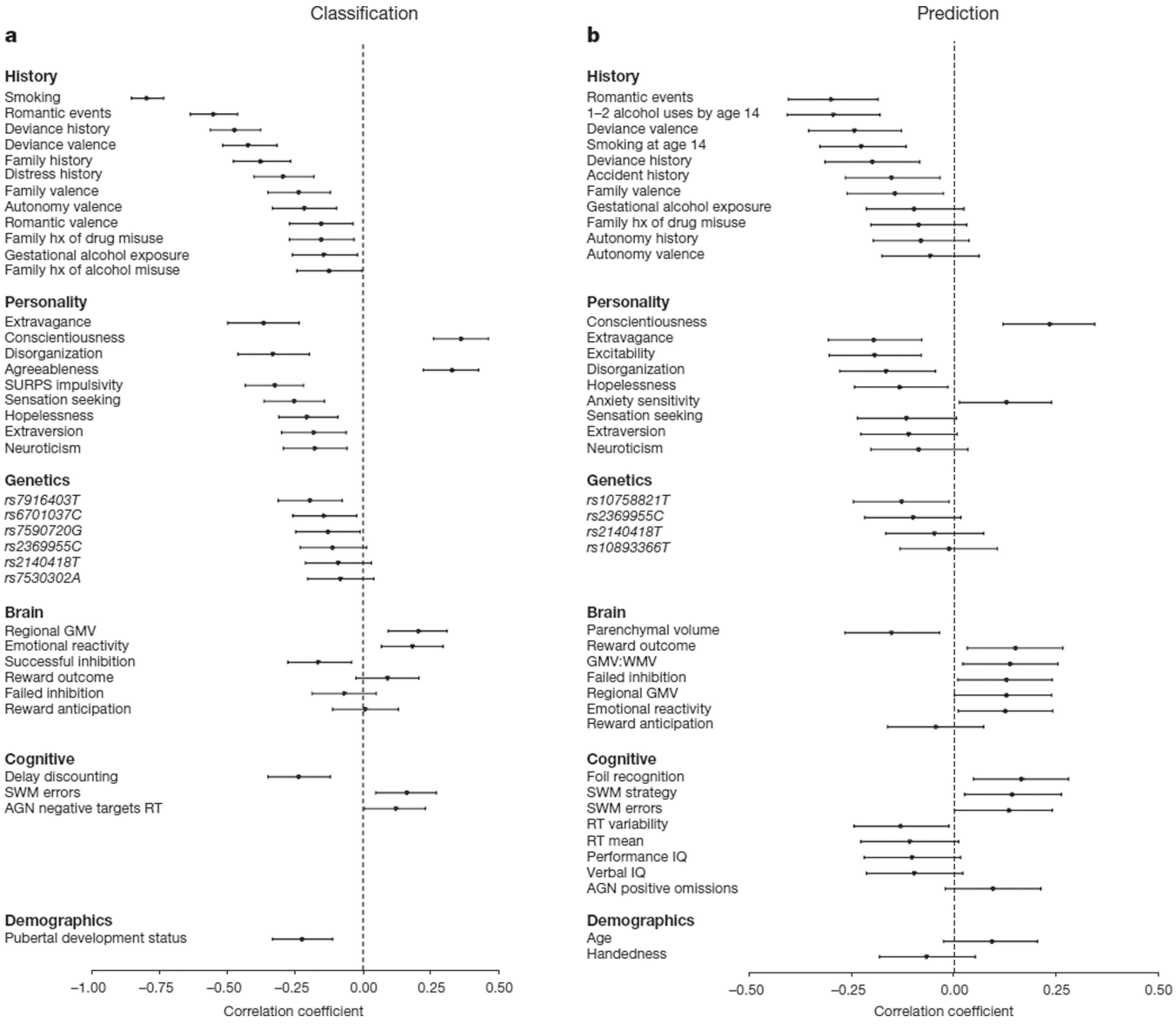

Figure 1. The relationship between group membership and each feature that was present in at least 9 folds of the final model

Position on the horizontal represents the point-biserial correlation statistic (*r*) between each feature and group membership. Negative *r* values indicate that higher scores are associated with an increased likelihood to engage in binge drinking at 14. Error bars represent 95% confidence intervals (calculated using 10,000 bootstraps). **a**, Analyses 1 and 2, the classification of binge drinking at age 14 years ($n = 265$). **b**, Analysis 8 predicting binge drinking at age 16 years ($n = 271$). AGN, affective go/no go; hx, history; SURPS, substance use risk profile scale; SWM, spatial working memory; GMV, grey matter volume; WMV, white matter volume.

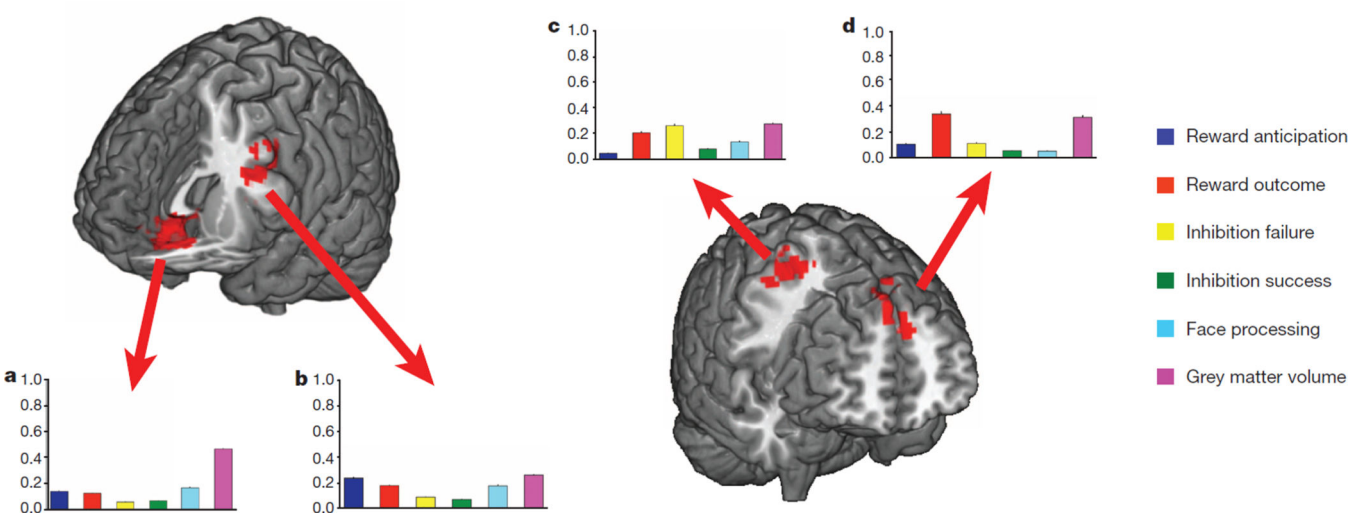

Figure 2. Brain regions associated with binge drinking and the relative contribution of each brain metric to the classification

The average beta weight for each brain metric (normalized to sum to 1 and averaged over the ten outer folds). Error bars depict standard errors of the mean across the folds. **a, b**, Brain regions that classify binge drinking at age 14, Analyses 1 and 2 (*n* = 265). The most robust brain classifiers were in ventromedial prefrontal cortex (**a**) and the left inferior frontal gyrus (**b**). **c, d**, Brain regions that predict binge drinking at age 16, Analysis 8 (*n* = 271). The most robust brain predictors of future binge drinking were the right precentral gyrus (**c**) and bilateral superior frontal gyrus (**d**).